Above Threshold Coulomb Explosion of Molecules in Intense Laser Pulses

B. D. Esry, A. M. Sayler, P. Q. Wang, K. D. Carnes, and I. Ben-Itzhak
J. R. Macdonald Laboratory, Kansas State University, Manhattan, Kansas 66506, USA
(Received 24 March 2006; published 5 July 2006)

We have measured and explained a new mechanism of molecular ionization near the appearance intensity that produces a sequence of peaks in the nuclear kinetic energy spectrum separated by the photon energy. Our interpretation is based on an internally consistent model for the nuclear motion during an intense laser pulse. Within this model, the same concepts and language can be used for both dissociation and ionization, leading to a more unified understanding of the dynamics.

DOI: 10.1103/PhysRevLett.97.013003 PACS numbers: 33.80.Rv

The ionization and dissociation of simple molecules in intense laser pulses has been studied for many years [1–3]. While much is understood, a model that describes the nuclear dynamics for both processes on an equal footing is still lacking. Even more useful would be a model with predictive power that is simple to apply. We will describe such a model below and present our experimental data to support it. Through the combination of the two, we identify a new feature in molecular breakup: above threshold Coulomb explosion (ATCE).

For concreteness, our discussion will focus on the simplest molecule, H_2^+, in a linearly polarized laser field, but the essential ideas and benefits of our model should generalize to more complicated systems. H_2^+ has the advantage that most of its properties can be calculated from first principles, making it a prime test bed for model development and comparison. Fortunately, experiments using H_2^+ beams have recently become available [4–7].

Some of the mechanisms of dissociation and ionization in H_2^+ are well understood [1–3]. To those in the field, the names are familiar: bond softening (BS), bond hardening (BH), above threshold dissociation (ATD), and charge-resonance enhanced ionization. For the uninitiated, the essential physics behind these names is simple. Bond softening simply describes the fact that a molecule's bond "softens" in an intense laser and the molecule comes apart. Bond hardening describes the counterintuitive result that high-lying vibrational states live longer than expected given their weaker binding. In above threshold dissociation, the molecule absorbs more photons than needed to dissociate, leading to signature peaks in the kinetic energy release (KER) spectrum separated by a photon's energy. All three of these mechanisms describe the dissociation of H_2^+ into $p + H$. They are most often explained using adiabatic Floquet potentials [8], that is, Born-Oppenheimer potentials that take into account the interaction with the laser field. The laser induces couplings and avoided crossings familiar from normal Born-Oppenheimer potentials, allowing the same methods of interpretation.

Charge-resonance enhanced ionziation, on the other hand, describes breakup into $p + p + e^-$, which we will label ionization. This mechanism [3] is an extension of the atomic tunneling picture of strong field ionization [2] to H_2^+. The two-center nature of H_2^+, however, is a nontrivial change and leads to enhanced ionization at particular internuclear distances. This picture is appropriate in the limit of low laser frequencies or high laser intensities.

What "low" and "high" actually mean in this context is usually quantified via the Keldysh parameter [2] $\gamma = \sqrt{E_b/2U_p}$ where E_b is the electronic binding energy. The ponderomotive energy U_p is the cycle-averaged energy of a free electron in the laser field and is proportional to I/ω^2, where I is the laser intensity and ω is its carrier frequency. When $\gamma \gg 1$, the system is said to be in the "multiphoton regime"; and when $\gamma \lesssim 1$, in the "tunneling regime". Key to our discussion is that there is no explicit reference to photons in the latter picture while there is in the former. The separation of intense laser-matter interactions into two regimes constitutes more a guideline than a hard-and-fast rule. In fact, each picture is sometimes useful in the other regime, and both can be useful for $\gamma \approx 1$. We note, in particular, that the standard description of H_2^+ dissociation in terms of the adiabatic Floquet potentials is fundamentally a multiphoton one, while the enhanced ionization picture is based on tunneling. In typical H_2^+ experiments [4–7], with a wavelength of 790 nm and intensities in the 10^{14}–10^{15} W/cm^2 range, γ hovers within about a factor of 2 of unity for the whole range of internuclear distance R.

In this Letter, we will present a model that describes both dissociation and ionization from a multiphoton point of view. Such a description seems likely to yield an interpretation complementary to that based on tunneling in this $\gamma \approx 1$ regime. Moreover, since experimental spectra include contributions from a range of intensities due to the variation of intensity within the laser focal volume, lower intensities—because they occur in a larger volume—tend to dominate, moving γ closer to the multiphoton regime. Stated another way, our model should work best for ionization at intensities near the appearance intensity.

The essence of our model is to reduce the problem, as much as is possible, to effective Born-Oppenheimer potential curves so that we can understand the dynamics in terms

of simple curve crossings. In a nutshell, we accomplish this using Floquet potentials that include the laser field by adding an extra index representing the number of photons to the field-free Born-Oppenheimer potentials.

In H_2^+, for example, the $1s\sigma_g$ state with no photons couples to the $2p\sigma_u$ state with one absorbed photon, which couples to the $1s\sigma_g$ state with two absorbed photons, and so on. Transitions due to the laser-induced coupling are most likely where curves cross. In general, the coupling between a curve with n photons and one with m is given roughly by $(\mathcal{E}D)^{|n-m|}$ where $\mathcal{E}$ is the electric field amplitude and D the dipole matrix element. Figure 1(a) shows the diabatic Floquet potentials typically used to describe BS, BH, and ATD. Bond softening is dissociation from the initial $1s\sigma_g - 0\omega$ state via the one-photon crossing to the $2p\sigma_u - 1\omega$ state. Any vibrational population near this crossing will preferentially dissociate. Higher vibrational states can also dissociate, but have some probability of staying on the $1s\sigma_g - 0\omega$ curve (BH). Lower vibrational states cannot dissociate via the one-photon crossing, but can exit through the three-photon crossing, leading to ATD.

Even though Floquet potentials assume a laser continuously on, we can introduce the time dependence of the laser pulse through the coupling elements [8]. So, the potentials of Fig. 1(a) hold throughout the pulse, but the couplings between the curves change with the pulse envelope. For example, a wave packet that starts in the $1s\sigma_g - 0\omega$ curve must reach the one-photon crossing during the pulse to make a transition. Having made that first transition, it must also reach the next crossing during the pulse, and so on.

We introduce the Born-Oppenheimer curves representing ionization in a manner exactly analogous to the dissociation curves. While these curves in principle represent the whole continuum of possible photoelectron energies, for the purposes of our model, we only draw the curve representing the field-free ionization threshold. Upon inclusion of the photon label, these ionization threshold curves, $1/R - n\omega$, cut across the dissociation curves as shown in Fig. 1(b). Note that dipole selection rules do not restrict these curves since continuum electron states

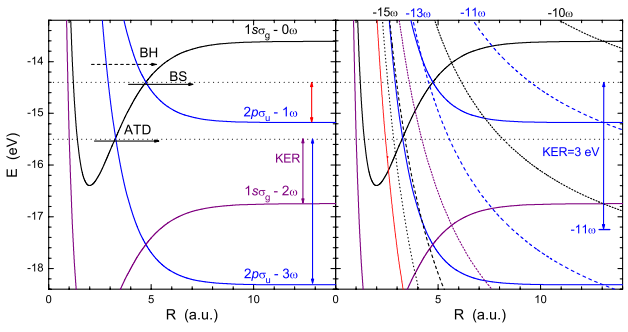

FIG. 1 (color online). (a) The diabatic Floquet potentials for H_2^+. Besides the molecular quantum numbers, each curve carries a photon number label. (b) The same as (a), but including the ionization threshold potentials.

of all symmetries exist at each energy. These ionization threshold potential curves can be viewed as an analogy to the Floquet picture, or they can be viewed as simply a convenient way to count photons. In our model, however, all photon counting—whether for dissociation or ionization—is carried out in exactly the same way.

It is clear from Fig. 1(b) that critical values of R occur where the ionization threshold potentials cross the dissociation potentials. We expect that these crossings, where the ionization channels open, will correlate to enhancements in the KER spectrum of the nuclei. By their nature, these channel openings are quasistationary with respect to intensity and will thus be emphasized in the intensity average inherent in experiments, thereby justifying our inclusion of only the ionization threshold curves. Many of these crossings can be interpreted as a manifestation of resonantly enhanced multiphoton ionization (REMPI). In fact, Madsen and Plummer [9] have shown that REMPI does enhance the ionization rate at critical R values in nonperturbative Floquet calculations for H_2^+. Our model thus predicts structure in the KER spectrum for laser intensities near the ionization appearance intensity. Further, we expect this structure to disappear as the intensity is increased since the coupling gets stronger, driving transitions over a wider range of R, yielding broader KER peaks.

To determine which crossings in Fig. 1(b) are most important, we use two general principles. First, among the transitions possible, those requiring the fewest number of photons will dominate. Second, the pulse should be long enough for the nuclei to reach the crossing while the pulse is intense enough to drive the transition (the nuclei in H_2^+ take about 2.7 fs to move 1 a.u. with 1 eV of kinetic energy). Both of these principles are necessarily more qualitative than quantitative, describing the trends to be expected. To be more specific, the positions of KER peaks can be predicted quantitatively from the curves, but their relative widths and intensities can only be predicted qualitatively. Nevertheless, given a particular experimental spectrum, we can predict how it will change with the laser parameters. In addition, we can predict the angular distribution of the nuclear fragments for each KER peak from the number of photons.

In our model, then, dissociation and ionization of H_2^+ in a 790 nm, $\gtrsim 10^{14}$ W/cm^2 laser pulse is initiated by BS on the rising edge of the pulse as the intensity grows past a few 10^{12} W/cm^2. The resulting dissociating wave packet has a mean total energy of around -14.4 eV, determined from the energy of the one-photon crossing. Ionization can then occur at the crossings with the 13ω through 10ω ionization channels, leading to peaks in the KER spectrum whose energies are determined from the difference between the total energy and the asymptotic thresholds of the various ionization curves. In fact, these peaks form a sequence separated by $\hbar\omega$, and are the result of a qualitatively new mechanism for molecular breakup. Extending existing nomenclature, we label this mechanism above threshold Coulomb explosion.

Ionization at the 13ω crossing can occur if the pulse intensity ramps up fast enough. This requirement is less restrictive than it might appear since the wave packet's velocity decreases substantially in this crossing. The resulting peak will likely be fairly broad and shifted lower from 6.1 eV—possibly to the $2p\sigma_u - 1\omega$ asymptotic threshold—due to the strong $1s\sigma_g - 0\omega$ to $2p\sigma_u - 1\omega$ coupling in the BS step. This effect is clear in the adiabatic Floquet potentials which have an avoided crossing whose gap is proportional to the electric field. This argument also leads to the general conclusion that the low-KER peaks from large-R crossings will tend to be sharper.

As the wave packet continues along the $2p\sigma_u - 1\omega$ potential, it encounters the 12ω crossing at $R = 7$ a.u. after about 8.5 fs. The wave packet still has a mean total energy of roughly -14.4 eV which translates into 0.68 eV of kinetic energy that it will keep if it ionizes. For pulses in the tens of femtoseconds range, we can expect this peak at 4.5 eV to be larger than the 13ω peak since the intensity will be closer to its maximum value at this crossing. Moreover, its KER might also be shifted from the BS step, but not by as much as the 13ω peak since any wave packet reaching this crossing was likely created earlier in the pulse at a lower intensity. Roughly 23.5 fs after dissociating, the wave packet reaches the 11ω crossing. If sufficient intensity remains, a transition can occur, giving rise to a 3.0 eV peak which should show even less KER shift. Transitions to the 10ω channel are possible but occur at much larger R ($\approx$45 a.u.), making them much less likely. We expect, then, that the shorter the laser pulse, the higher the KER on average.

Bond softening is not the only process that can initiate ionization. Figure 1(b) shows crossings with ionization curves at energies above the one-photon crossing. These crossings are accessible via BH. That is, only the high-lying vibrational states that do not decay immediately by BS will have any amplitude at the large R values of these crossings, favoring the $1s\sigma_g - 0\omega$ crossings near the outer turning points over the $2p\sigma_u - 1\omega$ crossing near $R = 4$ a.u.

Ionization can also be initiated by ATD. The resulting wave packet follows the $2p\sigma_u - 3\omega$ curve initially, but takes the adiabatic path to the $1s\sigma_g - 2\omega$ curve for even small intensities. Its average kinetic energy is much higher than for BS, though, so that it reaches the 12ω crossing near $R = 12.5$ a.u. in about the same time that the BS wave packet reaches this same R. The initial dissociation, however, is delayed from the single-photon process since it requires higher intensity. Ionization following ATD generates another sequence of ATCE peaks corresponding to 15ω through 12ω ionization. Again, based on time and intensity arguments, we expect the middle two peaks to be the larger of the four and the high-KER peaks to be shifted more than the low-KER peaks.

We now test our predictions by direct comparison with experiment. Figure 2 shows KER spectra that we have obtained using coincidence 3D molecular dissociation imaging of an H_2^+ beam [7,10] along with bars representing our predicted peak locations. The data was taken with 45 fs, 790 nm pulses at two intensities—one near the appearance intensity and the other about 2 times larger. We note that even with the relatively low statistics in Fig. 2(a), structure can be reliably identified. This structure disappears with increasing intensity [compare Fig. 2(a) and 2(b)] as expected from the peak broadening arguments given above. To quantify this test, we fit the KER distributions in Figs. 2(a) and 2(b) with a sum of four Gaussians. The fit was not completely free; rather, it was restricted using information from our model: the Gaussians were centered at the predicted locations and shared a common width. Where there were multiple pathways leading to the same KER ($\pm$0.2 eV), the Gaussian combines the peaks and has a larger width. The same positions were then used in Fig. 2(b) with the widths scaled larger by a factor to account for intensity broadening. Thus, between the two panels, there were effectively only 12 free parameters instead of 24. The quality of the fits suggests that our model does indeed have descriptive and predictive powers.

While the abundance of crossings makes a one-to-one, peak-to-pathway identification difficult, the 3 eV peak in Fig. 2(a) can be clearly associated with a single crossing: the 11ω crossing with the $2p\sigma_u - 1\omega$ curve. The source for the second prominent peak, at 3.8 eV, likely includes contributions from BH, BS (shifted by strong one-photon coupling), and ATD initiated mechanisms. The fact that we see any evidence of a BH initiated process is surprising since the population of the highly excited vibrational states is only a few percent in the nearly Franck-Condon distribution expected for the H_2^+ beam. Apparently, though, these states survive to an intensity high enough to drive their 11 photon ionization. The 4.8 eV peak is also likely a combination of peaks, this time from 12ω ionization of the BH states and 13ω ionization following ATD. Never-

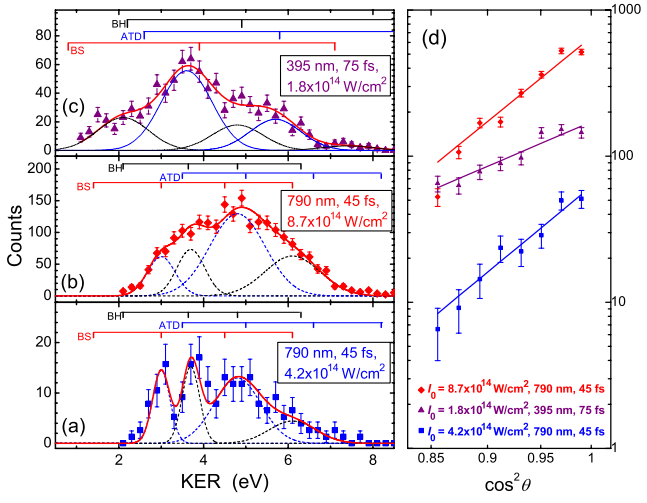

FIG. 2 (color online). (a)–(c) Experimental ionization KER spectra. The vertical bars indicate the predicted KER peak locations, grouped by initiating mechanism. (d) Experimental log-log angular distributions corresponding to the spectra (a)–(c).

theless, the structure in these spectra does match our predictions above, including ATCE. The exception is the peaks arising from the BH pathway—which our model did predict, but we did not expect to be measurable.

Looking again at Fig. 2, we see that the distribution shifts towards higher KER as the intensity increases. This trend has a natural explanation in our framework: these high-KER peaks require more photons and thus higher intensity. In fact, the highest KER peak expected from Fig. 1, at 8.2 eV, does not appear in Fig. 2 . Although not shown, we have seen experimentally that doubling the intensity from that in Fig. 2(b) to 1.7×10^{15} W/cm^2 does indeed yield a small, but clear, contribution at 8.2 eV. Interestingly, at this intensity, there is no similarly clear contribution from the direct 14-photon ionization from the $1s\sigma_g - 0\omega$ curve at 7 eV, even though it requires one fewer net photon. In our model, this is just a consequence of the enhanced transition probability due to the near degeneracy of the 15ω curve with the $2p\sigma_u - 3\omega$ curve.

Our model allows another prediction: the angular distribution of the nuclear fragments. An n-photon parallel transition—which we are assuming for both ionization and dissociation in H_2^+—gives a $\cos^{2n}\theta$ distribution. So, for ionization initiated by BS, we expect primarily 11 to 13 photon ionization; for ATD, 11 and 12 photon ionization. Figure 2(d) shows the experimental angular distributions. The distributions are plotted so that the expected $\cos^{2n}\theta$ behavior appears as a straight line. The data indeed fall nicely along a straight line with n lying between 12 and 13 in agreement with our prediction.

Our model, then, is consistent with our experimental data for 790 nm. To be truly useful, however, it should afford clear predictions and suggest experiments to test them. We have already shown tests of the predicted intensity and angular dependence, and we have mentioned that short laser pulses should give higher KER peaks than long pulses. The other fundamental laser parameter that can be relatively easily changed is the carrier frequency. If we consider a frequency-doubled Ti:sapphire laser, produce a set of potentials analogous to Fig. 1(b), and apply the same kind of analysis discussed above, then our model predicts that the angular distribution should have a 6–7 photon character with the primary KER peaks at around 2.2 eV (BH), 3.8 eV (BS), and 5.7 eV (ATD).

With these predictions in hand, we returned to the lab. The measured angular distribution, shown in Fig. 2(d), gives a $\cos^{2n}\theta$ fit with $n = 6.6 \pm 1.0$, in good agreement with our prediction. The KER spectrum is shown in Fig. 2(c) and also agrees well. In fact, it shows an even clearer low-KER, BH initiated peak. Unlike the 790 nm case, the KER structure for 395 nm can be readily associated with specific pathways since the higher photon energy leads to a comparative sparsity of crossings. The main 3.8 eV peak, for instance, arises from a 6ω, large-R crossing with $2p\sigma_u - 1\omega$. We already mentioned that the 2.2 eV peak is initiated by BH, and it can be shown that the 4.8 eV peak is as well. The 5.7 eV peak comes mostly from six photon ionization of the $1s\sigma_g - 2\omega$ ATD curve. Finally, the small contribution visible above 7 eV is ionization to the 7ω curve initiated by BS and BH. We followed the same procedure to fit this spectrum as before, except that we allowed the centroid of the main feature to be a fit parameter. Not surprisingly, the fit yielded a small downward shift of about 0.2 eV from the expected 3.8 eV for this BS initiated process.

We have described a simple, self-consistent model for the nuclear dynamics in dissociation and ionization. It incorporates all of the interpretive power of the Floquet potentials for dissociation and extends the same power to ionization, enabling us to identify ATCE. Direct comparison with experiment shows that our model—which only requires plotting the relevant potentials—describes *many* aspects of ionization of H_2^+ in both 790 and 395 nm light. In particular, it affords the possibility of identifying the pathway a system traveled to ionization. Not all such identifications are unique, but changing the laser wavelength improved the situation greatly. One important feature of our model is that it has predictive power, giving the dependence on intensity, pulse length, and carrier frequency, among other things. As a consequence, our model can be used to design new experiments to resolve the ambiguous identifications. It is easy to imagine, for instance, using the timing information inherent in the potential curves to implement and interpret a pump-probe experiment. The pump-probe scheme could be used to control the transitions at particular crossings, giving clear pathway assignments. In closing, we note that our model can be applied to other molecules—just as the Floquest language has been used for dissociation in other molecules. In H_2, for instance, our model would predict a structure very similar to that shown here.

We thank Z. Chang for providing the intense laser beams. Work supported by the Chemical Sciences, Geosciences, and Biosciences Division, Office of Basic Energy Sciences, Office of Science, U. S. Department of Energy.

[1] A. Giusti-Suzor, *et al.*, J. Phys. B **28**, 309 (1995).
[2] J. H. Posthumus, Rep. Prog. Phys. **67**, 623 (2004).
[3] T. Zuo and A. D. Bandrauk, Phys. Rev. A **52**, R2511 (1995); T. Seideman, M. Yu. Ivanov, and P. B. Corkum, Phys. Rev. Lett. **75**, 2819 (1995).
[4] K. Sändig, H. Figger, and T. W. Hänsch, Phys. Rev. Lett. **85**, 4876 (2000).
[5] I. D. Williams *et al.*, J. Phys. B **33**, 2743 (2000).
[6] D. Pavičić, *et al.*, Phys. Rev. Lett. **94**, 163002 (2005).
[7] I. Ben-Itzhak, *et al.*, Phys. Rev. Lett. **95**, 073002 (2005).
[8] D. Telnov and S. I. Chu, Phys. Rep. **390**, 1 (2004).
[9] L. B. Madsen and M. Plummer, J. Phys. B **31**, 87 (1998).
[10] P. Q. Wang, *et al.*, Phys. Rev. A (to be published).